LANGMUIR

pubs.acs.org/Langmuir Article

Local Confinement Controls Diffusive Nanoparticle Dynamics in Semidilute Polyelectrolyte Solutions

Ali H. Slim, Ryan Poling-Skutvik, and Jacinta C. Conrad*

Cite This: *Langmuir* 2020, 36, 9153–9159 Read Online

ACCESS | Metrics & More | Article Recommendations | Supporting Information

ABSTRACT: We investigate the mobility of polystyrene particles ranging from 100 to 790 nm in diameter in dilute and semidilute sodium polystyrene sulfonate (NaPSS) solutions using fluorescence microscopy. We tune the polymer conformations by varying the ionic strength of the solution. The nanoparticle mean-squared displacements evolve linearly with time at all time scales, indicating Fickian diffusive dynamics. In solutions of high ionic strength, chains adopt a random walk conformation and particle dynamics couple to the bulk zero-shear rate viscosity, according to the Stokes−Einstein picture. In solutions of low ionic strength, however, particle dynamics nonmonotonically deviate from bulk predictions as polymer concentration increases and are not accurately predicted by the available models. These nonmonotonic dynamics directly correlate with the non-Gaussianity in distributions of particle displacements, suggesting the emergence of a local confining length scale as polyelectrolyte concentration increases.

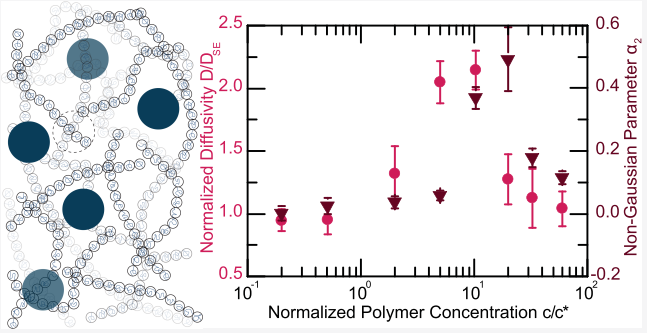

INTRODUCTION

Nanoparticle transport in concentrated complex fluids is important for enhanced oil recovery,[1,2] nanocomposite materials,[3,4] and targeted drug delivery.[5,6] Understanding the mechanisms controlling particle diffusion is necessary to enhance the efficacy of particle transport in these applications. The diffusion of a particle of radius R_{NP} in a homogeneous medium with viscosity η is given by the Stokes−Einstein (SE) equation, $D_{SE} = k_BT/6\pi\eta R_{NP}$. The assumptions underlying the SE model do not hold as the particle size becomes comparable to the length scales of inhomogeneities in the medium, and deviations from SE predictions appear.[7−10] In this size regime, particle dynamics depend on length scales present in solution.

In entangled solutions, the length scale controlling particle dynamics is the tube diameter a, the distance between entanglement strands. The entanglement mesh cages large particles until the time scale of reptation after which SE behavior is recovered.[11−14] Conversely, particles that are much smaller than the entanglement mesh diffuse through the mesh and are unaffected by the polymer network. In unentangled polymer solutions, however, particle dynamics are controlled by the correlation length ξ, the distance between neighboring chains. Hydrodynamic models assume polymer solutions to be a homogeneous medium in which hydrodynamic interactions decay over ξ[10,15,16] and in which particle dynamics are dictated by polymer length scales, such as radius of gyration R_g and ξ.[13,17,18] These pictures have been developed for neutral polymers. In charged polymers, by contrast, electrostatic repulsion between monomers alters the structure and chain flexibility.[19,20] The size of the charged group and its recurrence within the monomers results in conformations ranging from a rigid rod to a semiflexible chain. In turn, the local conformation determines the mesh geometry. As a result of these structural differences, the onset of entanglements in charged polymers is shifted to much higher concentrations than for neutral chains.[21,22] The pronounced differences in structure and relaxations in charged polymers likely affect the length scales controlling diffusive transport of nanoparticles. Despite recent studies of nanoparticle diffusion in charged polymer solutions and melts,[23,24] the effect of charge-induced conformation on nanoparticle transport remains incompletely understood.

Here, we probe the dynamics of nanoparticles in dilute and semidilute unentangled solutions of a model polyelectrolyte. The polymer conformation is tuned by varying the solution ionic strength. The particle dynamics are diffusive across all experimental time scales. We find that the diffusivity of large particles ($R_{NP}/R_g > 1$) follows bulk predictions at all ionic strengths. For smaller particles ($R_{NP}/R_g < 1$), however, we observe surprising dynamics with nonmonotonic deviations

Received: May 11, 2020
Revised: July 16, 2020
Published: July 17, 2020

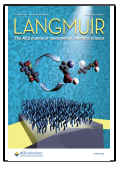

https://dx.doi.org/10.1021/acs.langmuir.0c01402
Langmuir 2020, 36, 9153−9159

from SE within the unentangled semidilute regime. The size-dependent dynamics do not collapse onto a master curve according to physical arguments derived for Gaussian chains. We find that the non-Gaussian parameter maps onto the same concentration dependence as scaled particle diffusivity D/D_{SE}, suggesting the rise of confinement effects despite the absence of entanglements.

MATERIALS AND METHODS

Solution Preparation. Glass vials were cleaned overnight in a solution of 6.5 wt % potassium hydroxide in isopropanol, ensuring near salt-free conditions. Vials were thoroughly rinsed 10 times using Millipore water to remove any residual salt and then dried in an oven at 105 °C for 2 h. Fluorescent polystyrene particles with diameters d_{NP} ranging from 100 to 790 nm (Fluoro-Max, Thermo Fisher Scientific) were dispersed in aqueous solutions of NaPSS with a weight-averaged molecular weight M_w = 2,200,000 Da (Scientific Polymer Products) at three different ionic strengths. A constant particle volume fraction $\phi = 1.5 \times 10^{-6}$ was used across all samples to minimize interparticle interactions and avoid aggregation (observed for $\phi \geq 1.5 \times 10^{-5}$) while maintaining good statistics for particle tracking. Deionized water was assumed to have an ionic strength of 10^{-6} M,[25] whereas the other two sets of samples were prepared using sodium chloride to achieve ionic strengths of 10^{-3} and 10^{-1} M. The overlap concentration c^* of NaPSS was estimated at each ionic strength from intrinsic viscosity measurements (Supporting Information), and the radius of gyration $R_{g,0}$ in each ionic strength solution was determined via $R_{g,0} = (M_w/(4/3\pi N_{av}[\eta]))^{1/3}$.[26,27] The resulting $R_{g,0}$ values in dilute solutions were 190, 130, and 75 nm at ionic strengths of 10^{-6}, 10^{-3}, and 10^{-1} M, respectively.

Bulk Rheology. Steady-shear measurements of the rate-dependent viscosity were performed on a Discovery Hybrid Rheometer (TA Instruments, HR-2). Polymer solutions were loaded into a single-gap Couette cell with a cup diameter of 15 mm, a bob diameter of 14 mm, and a bob length of 42 mm. The inertia and torque of the instrument were calibrated prior to measurements. Samples were presheared for 1 min to reach equilibrium after which the viscosity was determined as the average value over 1 min.

Imaging Sample Preparation. To create a sample chamber for imaging, two cover slips (22 mm × 22 mm × 0.2 mm, Fisherbrand cover glass) were adhered on a Gold Seal cover glass (48 mm × 65 mm × 0.15 mm) using a UV epoxy-based adhesive to form two sides of a chamber. Another cover slip was attached on top of the two cover glass slips using UV epoxy. The particle−polymer solutions were then pipetted through one of the two open sides. Finally, the two remaining open sides were sealed with UV epoxy.

Imaging and Particle Tracking. A Leica DM4000 inverted fluorescent microscope equipped with 63× and 100× oil immersion lenses was used to acquire a series of images of quiescent samples over time. For each image series, 4100 images were captured at a frame rate of 32 fps. At least five image series per sample were recorded at different locations. Particle centroids were located with spatial resolutions of 25 and 35 nm for 200 and 790 nm particles, respectively, and tracked over time using particle tracking algorithms.[28] From the particle trajectories, we calculated the one-dimensional ensemble-averaged mean-squared displacement (MSD) $\langle \Delta x^2(\Delta t) \rangle$ as a function of lag time Δt. At least 10^4 time steps were averaged for each MSD data point. To extract the diffusivity D, we fitted each MSD to $\langle \Delta x^2(\Delta t) \rangle = 2D\Delta t$.

RESULTS AND DISCUSSION

We characterize the rheological properties of the polyelectrolyte solutions at three solution ionic strengths. The viscosity increases concomitant with polymer concentration c/c^* and is approximately independent of the shear rate across 2 orders of magnitude in concentration (inset of Figure 1), indicating that the chains relax quickly in solution (10^{-3} and 10^{-1} M shear viscosity in the Supporting Information).

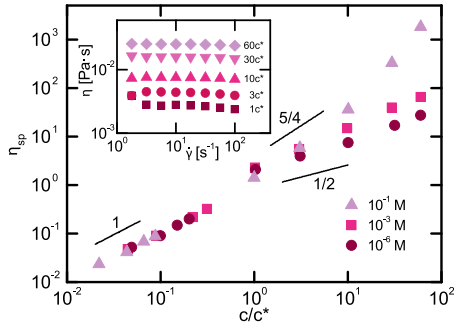

Figure 1. Specific viscosity $\eta_{sp} = (\eta - \eta_0)/\eta_0$ as a function of normalized NaPSS concentration c/c^* for solutions of various ionic strengths. Inset: viscosity η for 10^{-6} M ionic strength solutions as a function of shear rate $\dot{\gamma}$. Bottom and top solid lines represent viscosity scaling predicted for polyelectrolytes in the limit of low and high ionic strength, respectively.

The viscosity of charged polymer solutions exhibits a dependence on ionic strength that is not observed for their neutral counterparts.[22,29] We examine the changes in specific viscosity $\eta_{SP} = (\eta - \eta_0)/\eta_0$ because it offers a direct measurement of the polymer contribution to solution viscosity. The specific viscosity of the polyelectrolyte solutions increases as a function of both polymer and ionic strength. In the dilute regime, the specific viscosity scales with concentration as $\eta_{sp} \sim (c/c^*)^1$ following the theoretical prediction.[30] The specific viscosity is independent of ionic strength for concentrations $c/c^* < 1$ due to the dominance of hydrodynamic interactions.[31,32] In the semidilute regime ($c/c^* > 1$), the specific viscosity scales according to predictions[30] for polyelectrolyte solutions at low ($\eta_{sp} \sim (c/c^*)^{1/2}$) and high ($\eta_{sp} \sim (c/c^*)^{5/4}$) ionic strength.[21,22,30] When the ionic strength is intermediate between these limits, however, the specific viscosity in the semidilute regime scales with concentration as $\eta_{sp} \sim (c/c^*)^{\alpha}$ with $\alpha = 0.8 \pm 0.1$. The specific viscosity increases with ionic strength for constant c/c^* in the semidilute regime, consistent with an increase in chain−chain interactions as the salt screens monomeric repulsion.[22] We observe a sharp upturn in η_{sp} at high polymer concentrations only in solutions of high ionic strength, suggesting that these solutions are entangled. Such a crossover, however, is not observed at low and intermediate ionic strength, suggesting the absence of chain entanglements. These observations are consistent with the expectations for entanglements in charged polymer solutions occurring at high concentrations that are $\gg 10c^*$.[22] Thus, these polyelectrolyte solutions have rheological properties that agree well with existing theories[21,25,30] and serve as a model system to investigate how particle dynamics depend on polymer conformations.

The mobility of nanoparticles in polyelectrolyte solutions decreases with increasing nanoparticle size (Figure 2a) and polymer concentration (Figure 2b). The mean-square displacement (MSD) scales linearly with the lag time $\langle \Delta x^2 \rangle = 2D\Delta t$ across all time scales, indicating diffusive dynamics with a diffusivity D as expected for Newtonian solutions with fast relaxations. We remove explicit size dependence by normalizing D by the diffusivity of the particle in pure solvent D_0.

https://dx.doi.org/10.1021/acs.langmuir.0c01402
Langmuir 2020, 36, 9153−9159

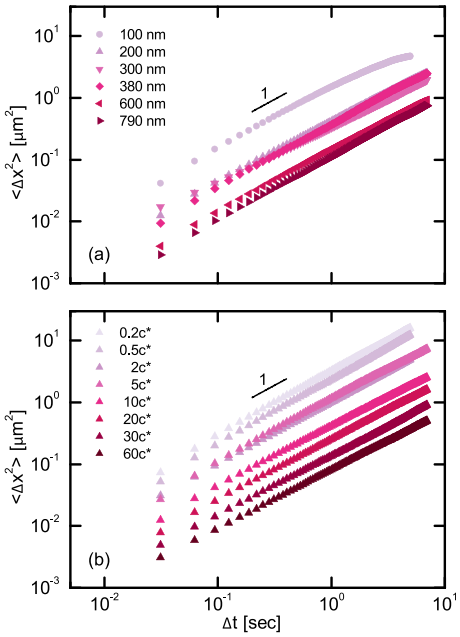

Figure 2. Mean-square displacement (MSD; $\langle \Delta x^2 \rangle$) as a function of lag time Δt for (a) particles of various sizes in a solution of polymer concentration $10c^*$ and (b) for 200 nm particles in solutions of various polymer concentrations. The ionic strength is 10^{-6} M (MSDs at 10^{-3} and 10^{-1} M ionic strength can be found in the Supporting Information). Solid lines represent linear scaling.

Particles diffuse according to solvent viscosity at low polymer concentrations across all ionic strengths $D/D_0 = 1$ (Figure 3). The dynamics slow down as concentration increases into the semidilute regime. At a given concentration c/c^* within the semidilute regime, the particle dynamics are faster as the ionic strength decreases, consistent with the lower viscosity of the solutions (Figure 1). The normalized diffusivities are approximately independent of the particle size in solutions of ionic strengths of 10^{-1} and 10^{-3} M, consistent with the idea that the particle diffusion probes the bulk solution viscosity. In solutions with the lowest ionic strength (10^{-6} M), however, the dynamics of small particles deviate from those of large particles, indicating that the dynamics of small particles decouple from the bulk solution viscosity.

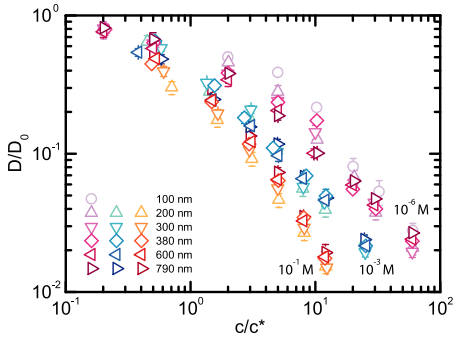

Figure 3. Normalized particle diffusivity D/D_0 as a function of polymer concentration c/c^* in solutions of different ionic strengths. Error bars represent the standard deviation of five measurements per sample.

To quantify the extent to which dynamics deviate from the predictions using bulk solution viscosity, we examine the particle diffusivity normalized by the Stokes−Einstein diffusivity D/D_{SE} as a function of polymer concentration. We use the dynamics of the large particles to quantify bulk solution viscosity so that $D_{SE}/D_0 = D_{790}/D_{790,0}$ to overcome torque limitations of the rheometer at low solution viscosity. Particles in solutions of high (10^{-1} M) and intermediate (10^{-3} M) ionic strength exhibit diffusivities that approximately conform to the Stokes−Einstein prediction using the measured bulk viscosities (Figure 4a,b). We attribute systematic deviations in D/D_{SE} from the predicted value of 1 to the use of the largest particles as bulk probes. In these solutions, the particles are larger than the radii of gyration of the polymers at infinite dilution, which we calculate to be 130 and 75 nm for solutions of intermediate (10^{-3} M) and high (10^{-1} M) ionic strength. Thus, the near-Stokes−Einstein diffusivities measured for which $R_{NP} > R_g$ are consistent with earlier studies that show that the dynamics of large particles ($R_{NP} > R_g$) couple to bulk viscosity behavior, according to the SE prediction.[33]

By contrast, the dynamics in solutions at low ionic strengths (10^{-6} M) depend on the particle size. The diffusivities of 600 nm particles follow the predicted SE behavior at all polymer concentrations (Figure 4c). The dynamics of smaller particles, however, agree with SE predictions at low polymer concentrations ($c/c^* < 1$) but exhibit a striking departure from SE predictions at higher polymer concentrations. This deviation increases with increasing polymer concentration until $c/c^* \approx 10$ at which point the particle dynamics begin to approach SE predictions again. In these low ionic strength solutions, the particles are comparable in size to the radius of gyration of the polymer ($R_{NP} \sim R_g$), and hence, the solutions cannot be treated as homogeneous continua. In this limit, interactions between particles and polymer chains become more important and lead to deviations from predictions based on the bulk solution rheology.[13,34]

A number of models and scaling theories attempt to explain particle dynamics in polymer solutions. Empirical models generally fall into one of two categories: obstruction[35−40] or

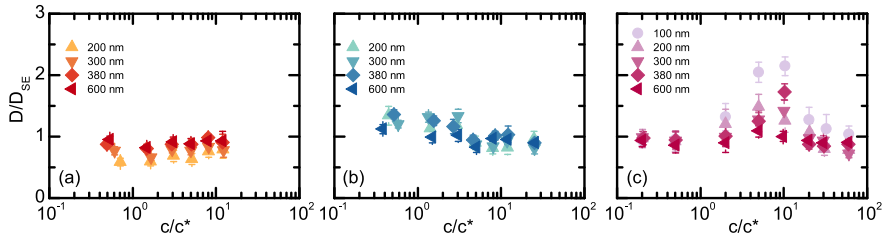

Figure 4. Diffusivity normalized to SE predictions D/D_{SE} as a function of polymer concentration c/c^* at (a) 10^{-1}, (b) 10^{-3}, and (c) 10^{-6} M ionic strength. Error bars represent the standard deviation of five measurements per sample.

https://dx.doi.org/10.1021/acs.langmuir.0c01402
Langmuir 2020, 36, 9153−9159

hydrodynamic.[10,15,16,34,41−43] Obstruction models assume that the polymer mesh is effectively immobile on time scales of particle diffusion and serve as geometric barriers to particle diffusion, but this assumption does not hold in our system because chains relax on time scales of the same order of magnitude as those characterizing the particle dynamics (Supporting Information). Hydrodynamic models assume that hydrodynamic interactions are screened over ξ so that viscous drag increases as ξ decreases. Hydrodynamic models, however, predict monotonic deviations from Stokes−Einstein behavior because ξ decreases monotonically with increasing polymer concentration. Importantly, these empirical models cannot describe the nonmonotonic behavior of D/D_{SE} in our system.

A second category of models incorporate how the particle interacts with the polymer. For neutral polymer systems, the polymer may develop a depletion layer around the particle, whereas for attractive polymer systems, the surrounding polymer will form a bound layer covering the particle. In the depletion layer picture, the particle diffuses quickly through the depletion layer and then slowly through the polymer mesh.[34] Our data, however, does not collapse according to the scaling suggested by this picture (Supporting Information), suggesting the absence of a depletion layer surrounding the particles. In the bound layer picture, the polymer binds to the surface of the particle and increases the viscous drag acting on the particle so that the particle diffusion is slower than expected.[44] Dynamic light scattering (DLS) on our particles in NaPSS solutions in the low and high ionic strength limits and in dilute conditions reveal that polymer chains do not significantly adsorb on the particle (Supporting Information). Moreover, we expect that particles with a bound layer would exhibit slower-than-expected diffusion, whereas in our experiments, D/D_{SE} approaches 1 for solutions with high polymer concentrations and low ionic strength.

A third class of pictures, developed for particles in dielectric media, predict a nonmonotonic decrease in the diffusion coefficient when a particle is surrounded by an electric double layer of comparable size[45] or when the particle dielectric constant increases.[46] The former case[45] results in slowing down of particle diffusion when the particle size is on the order of the inverse of the Debye length (i.e., $d_{NP}\kappa = 1$ where κ^{-1} is the Debye length). Our experiments, however, span size ratios that are orders of magnitude larger than $2R_{NP}\kappa = 1$. Furthermore, ref 45 predicts that particle dynamics are slower at intermediate electrolyte concentrations ($-2 < \log(2R_{NP}\kappa) < 1$) before recovering SE behavior at higher electrolyte concentrations ($\log(2R_{NP}\kappa) > 1$) and hence trend in the opposite direction of our data. Finally, the predicted deviations from SE behavior are on the order of ∼10%,[45] which are much smaller than our observed deviations (Figure 4). The latter picture[46] predicts an enhanced polymer−particle affinity as the chain length or nanoparticle size increases when the dielectric constant of the particle increases beyond that of the surrounding medium. The polystyrene particles in our experiments, however, have a dielectric constant ($\varepsilon = 2.5$) that is significantly lower than the solvent, water ($\varepsilon = 80$). Additionally, we expect the negatively charged polystyrene particles and polyelectrolyte chains to further reduce the affinity of chains to adsorb on the particle surface. Thus, these models are also not able to describe the nonmonotonic deviations from SE dynamics in our low ionic strength samples.

A final model predicts that, within certain size ranges, the particle dynamics are coupled to the relaxations of polymer segments of similar size.[13] In this theory, particle−polymer coupling results in diffusion according to an effective solution viscosity that is lower than the bulk viscosity.[13] In our earlier experiments on partially hydrolyzed polyacrylamide, the coupling theory scaling prediction $D/D_0 \sim (R_{NP}/\xi)^{-2}$ was able to collapse the diffusivities of systems with similar particle−polymer size ratios (R_{NP}/R_g).[47] This scaling, however, is not able to collapse the diffusivities measured in NaPSS solutions onto a master curve (Supporting Information). This result suggests that different physics must control particle dynamics in these solutions as compared to a solution of fully flexible Gaussian chains, likely arising from effects due to the charge on the polymers in the semidilute regime.

To identify the controlling physics, we examine the differences between polyelectrolytes and uncharged polymers. Both the radius of gyration $R_g \sim c^{-1/4}$ and the correlation length $\xi \sim c^{-1/2}$ (calculations provided in the Supporting Information) of polyelectrolytes decrease as the concentration is increased (Table 1), similar to those for neutral chains but

Table 1. Calculated Correlation Length ξ and Radius of Gyration R_g as a Function of Polymer Concentration for Solutions of Varying Ionic Strengths Using the Scaling Theory[21,22,30]

c/c^*		1.5	2	5	10	20	30
10^{-6} M	ξ [nm]	164	121	68	44	28	22
	R_g [nm]	174	165	140	123	108	101
10^{-3} M	ξ [nm]	98	80	43	26	16	12
	R_g [nm]	122	117	102	91	82	7
10^{-1} M	ξ [nm]	94	43	21	12	7	
	R_g [nm]	72	70	63	59	55	

with different scaling exponents.[22,30,32] Surprisingly, we observe nonmonotonic behavior in D/D_{SE} when $R_{NP}/R_g < 1$ for all polymer concentrations (100 and 200 nm diameter particles), when $R_{NP}/R_g > 1$ for all polymer concentrations (380 nm), and when R_{NP}/R_g transitions from <1 to >1 as concentration is increased (300 nm). Likewise, we observe nonmonotonic behavior when $R_{NP}/\xi > 1$ for all concentrations (380 nm) and when R_{NP}/ξ transitions from <1 to >1 as concentration is increased (100, 200, and 300 nm). Thus, structural length scales do not directly control the nonmonotonic behavior of D/D_{SE} in the semidilute regime. Second, prior studies on NaPSS revealed that chain relaxation times exhibit a local maximum at the overlap concentration,[21] first increasing with concentration in the dilute regime and subsequently decreasing with concentration in the semidilute regime.[29,48] The nonmonotonic deviations from SE in our study do not occur at the crossover between dilute and semidilute regimes but rather well within the semidilute regime $c/c^* \sim 10$. This result suggests that the nonmonotonic behavior in D/D_{SE} in the semidilute regime does not arise from nonmonotonicity in the chain relaxation time.

Because length and time scales of the NaPSS do not directly control the nonmonotonic particle dynamics, we assess if local polymer properties may be controlling the particle behavior. The original scaling theory of Wyart and de Gennes[17,29] predicts that small particles (whose size is comparable to the polymer blob size) that exhibit faster-than-SE diffusion at low to moderate polymer concentrations experience macroscopic

https://dx.doi.org/10.1021/acs.langmuir.0c01402
Langmuir 2020, 36, 9153−9159

viscosity above a concentration $c_{limit}/c^* = (R/R_g)^{-4/3}$ in entangled solutions. In this picture, cages in an entangled polymer mesh constrain particles on time scales shorter than the reptation time scale after which SE behavior is recovered. Thus, the rise in entanglements with increasing concentration controls the transition from micro- to macroviscosity controlled diffusion. Indeed, nonmonotonic deviations from SE were reported for polystyrene spheres in solutions of poly(vinyl methyl ether).[49] Although physically appealing, this picture is not directly applicable to our experiments because the polymer solutions with low ionic strength are not entangled in the range of concentrations explored in this study (as determined through rheology; Supporting Information). Additionally, although the rheological measurements of the high ionic strength polymer solutions suggest that these solutions are entangled at high concentrations (Figure 1), they follow SE predictions across all investigated concentrations (Figure 4a). This comparison suggests that the chain entanglements do not significantly affect particle dynamics in this regime. Nevertheless, we are inspired by this picture to further examine the particle dynamics to look for signatures of local structural effects that may act like an entanglement-produced cage.

We hypothesize that the nonmonotonic dynamics may be associated with particles experiencing local heterogeneity in solution. The distributions of particle displacements $G_s(\Delta x, \Delta t) = \frac{1}{N}\langle\sum_{i=1}^{N}\delta(x_i(t) - x_i(t+\Delta t) - \Delta x)\rangle$ are Gaussian on all accessible time scales for some particle sizes and polymer concentrations (e.g., 100 nm particles and $2c/c^*$; Figure 5a). For 100 nm particles at $20c^*$, however, $G_s(\Delta x, \Delta t)$ is non-Gaussian for all accessible lag times (Figure 5b). For all samples, the non-Gaussian parameter $\alpha_2 = \frac{\langle\Delta r^4\rangle}{3\langle\Delta r^2\rangle^2} - 1$, which characterizes the extent to which the distributions deviate from the Gaussian prediction for Fickian diffusion, is approximately independent of time. Surprisingly, we find that α_2 for the 100 nm particles is also a nonmonotonic function of c/c^* and exhibits a local maximum (Figure 5c). Moreover, the concentration at which it attains its local maximum, $20c/c^*$, is close to that at which D/D_{SE} attains its local maximum, providing additional evidence that the nonmonotonic deviations from SE may be related to particles experiencing different heterogeneous environments.

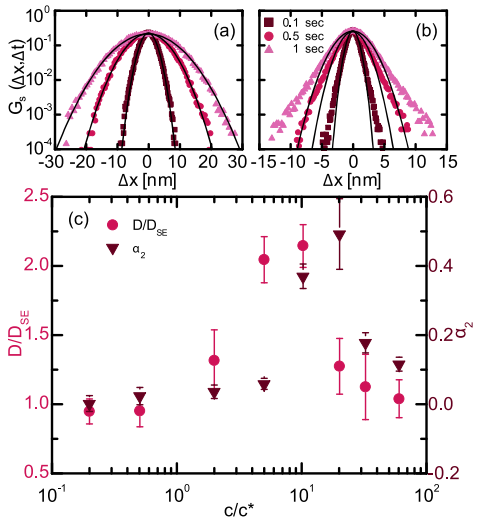

Figure 5. Normalized distribution of displacements G_s at various times for 100 nm particles in solutions of polymer concentrations (a) $2c^*$ and (b) $20c^*$ at a 10^{-6} M ionic strength. Solid lines represent Gaussian fits. (c) Scaled diffusivity D/D_{SE} and non-Gaussian parameter α_2 as a function of polymer concentration c/c^* for 100 nm particles at a 10^{-6} M ionic strength.

Non-Gaussian distributions of particle displacements can arise from temporal[50,51] or spatial[52,53] heterogeneities in the environment or from multiple dynamic modes.[54,55] In these solutions, chain relaxations occur on time scales faster than those characterizing particle diffusion (inset of Figure 1), indicating that the solution dynamics are not temporally heterogeneous on time scales relevant for particle diffusion. Anomalously large displacements are often attributed to hopping of particles between cages in a mesh or network.[56−58] A recent theory proposes that particles whose size is comparable to or slightly larger than ξ in entangled solutions experience intermittent hopping within the mesh at long time scales.[13,18] Recent experiments attribute the non-Gaussian behavior in entangled solutions to a competition between three time scales: the short-time relaxation of an entanglement strand, the time scale for activated hopping of nanoparticles, and the long-time reptation of the polymers.[57,59] In our experiments, however, the solutions are not entangled. Instead, we propose that the return to SE diffusion arises due to increasing confinement from the polymers. These confinements behave similarly to a tube diameter in an entangled system and become more prominent as the polymer concentration is increased. Because the nonmonotonic deviations from SE are not observed in the salted solutions, our results suggest that the anomalous diffusion in Figure 4 arises from the distinctive structural properties of polyelectrolytes.

To explore the confinement picture, we calculate displacement autocorrelation functions $C_d(t) = \langle\Delta x(t+\tau)\Delta x(t)\rangle$ at all polymer concentrations in 10^{-6} M solutions. The displacements of 100 nm particles become anticorrelated at $t = 32$ ms, which corresponds to the first time interval in our movies in solutions with $c > 10c^*$ (Figure 6). The degree of anticorrelation increases with increasing polymer concentration but decreases for larger particles (Supporting Information). The larger anticorrelation in 100 nm particles suggests that they experience caging-like effects in which the particle rebounds after encountering an elastic polymer network as polymer concentration increases. Additionally, the appearance

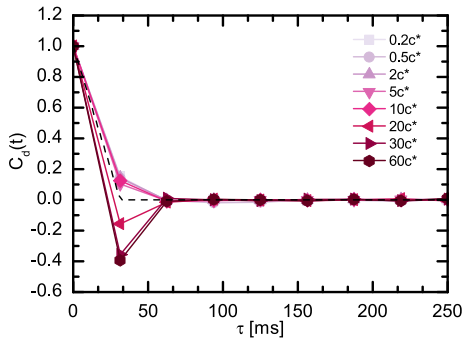

Figure 6. Normalized coefficient of displacement autocorrelation $C_d(t)$ as a function of elapsed time τ for 100 nm particles in NaPSS solutions at a 10^{-6} M ionic strength. The dashed line represents the displacement autocorrelation of a Gaussian process.

https://dx.doi.org/10.1021/acs.langmuir.0c01402
Langmuir 2020, 36, 9153−9159

of anticorrelated displacements occurs close to the onset of non-Gaussian particle displacements and the maximum in the D/D_{SE} deviation. Together, these factors suggest that the observed anomalous diffusion is a result of the unique structural properties of polyelectrolytes.

CONCLUSIONS

We probe the mobility of nanoparticles of a diameter of 100−790 nm in dilute and semidilute solutions of a model flexible polyelectrolyte, sodium polystyrene sulfonate, at three different ionic strengths (10^{-6}, 10^{-3}, and 10^{-1} M). We find that nanoparticles exhibit Fickian diffusion on experimental time scales with dynamics that become slower as the particle size and polymer concentration are increased. Large particles ($R_{NP} > R_g$) diffuse according to Stokes−Einstein predictions at all ionic strengths. The diffusivities of small particles ($R_{NP} < R_g$) in polyelectrolyte solutions of low ionic strength, however, exhibit a nonmonotonic deviation from the SE prediction that depends on polymer concentration, including a return to SE behavior at high polymer concentrations. Available models for diffusion of particles in solutions of fully flexible Gaussian chains are unable to explain the observed dynamics. In analogy with a physical picture developed for particle diffusion in entangled systems, we suggest that increasing constraints on particle motion due to confinement by the polyelectrolyte chains are responsible for the return to SE diffusion at high concentrations.

The length scale driving this confinement is still unknown. The polymer structure on short length scales may need to be considered to develop models that are capable of capturing particle dynamics in charged polymer solutions. To probe the dynamics of different size particles at the relevant size limit ($R_{NP} \ll R_g$), different dynamic techniques (such as but not limited to X-ray photon correlation spectroscopy (XPCS) or superresolution microscopy) are required to extend the dynamic range beyond the resolution limit of optical microscopy ($d_{NP} \sim 100$ nm). A better understanding of the length scales controlling particle dynamics has interesting implications for a wide range of applications requiring diffusion in complex media, including rigid rods,[60] emulsions,[61] and cellular cytoplasm.[42]

ASSOCIATED CONTENT

Supporting Information

The Supporting Information is available free of charge at https://pubs.acs.org/doi/10.1021/acs.langmuir.0c01402.

Supporting information regarding intrinsic viscosity, polymer length scales, time scales, dynamic light scattering, rheology, obstruction models, hydrodynamic models, and displacement autocorrelations (PDF)

AUTHOR INFORMATION

Corresponding Author

Jacinta C. Conrad − *Department of Chemical and Biomolecular Engineering, University of Houston, Houston, Texas 77204-4004, United States;* orcid.org/0000-0001-6084-4772; Email: jcconrad@uh.edu

Authors

Ali H. Slim − *Department of Chemical and Biomolecular Engineering, University of Houston, Houston, Texas 77204-4004, United States*

Ryan Poling-Skutvik − *Department of Chemical and Biomolecular Engineering, University of Pennsylvania, Philadelphia, Pennsylvania 19104, United States;* orcid.org/0000-0002-1614-1647

Complete contact information is available at: https://pubs.acs.org/10.1021/acs.langmuir.0c01402

Notes

The authors declare no competing financial interest.

ACKNOWLEDGMENTS

We thank Megan Robertson and Peter Vekilov for access to the rheometer and camera. This work was supported by NSF (CBET-1705968) and the Welch Foundation (E-1869).

REFERENCES

(1) Lin, Y.; Skaff, H.; Emrick, T.; Dinsmore, A. D.; Russell, T. P. Nanoparticle Assembly and Transport at Liquid-Liquid Interfaces. *Science* **2003**, *299*, 226−229.

(2) Bresme, F.; Oettel, M. Nanoparticles at fluid interfaces. *J. Phys.: Condens. Matter* **2007**, *19*, 413101.

(3) Winey, K. I.; Vaia, R. A. Polymer Nanocomposites. *MRS Bull.* **2007**, *32*, 314−322.

(4) Kashiwagi, T.; Du, F.; Douglas, J. F.; Winey, K. I.; Harris, R. H., Jr.; Shields, J. R. Nanoparticle networks reduce the flammability of polymer nanocomposites. *Nat. Mater.* **2005**, *4*, 928−933.

(5) Peer, D.; Karp, J. M.; Hong, S.; Farokhzad, O. C.; Margalit, R.; Langer, R. Nanocarriers as an emerging platform for cancer therapy. *Nat. Nanotechnol.* **2007**, *2*, 751−760.

(6) Tang, L.; et al. Investigating the optimal size of anticancer nanomedicine. *Proc. Natl. Acad. Sci. U. S. A.* **2014**, *111*, 15344−15349.

(7) Mackay, M. E.; Dao, T. T.; Tuteja, A.; Ho, D. L.; Van Horn, B.; Kim, H.-C.; Hawker, C. J. Nanoscale effects leading to non-einstein-like decrease in viscosity. *Nat. Mater.* **2003**, *2*, 762−766.

(8) Tuteja, A.; Mackay, M. E.; Narayanan, S.; Asokan, S.; Wong, M. S. Breakdown of the continuum Stokes-Einstein relation for nanoparticle diffusion. *Nano Lett.* **2007**, *7*, 1276−1281.

(9) Ye, X.; Tong, P.; Fetters, L. J. Transport of probe particles in semidilute polymer solutions. *Macromolecules* **1998**, *31*, 5785−5793.

(10) Cheng, Y.; Prud'homme, R. K.; Thomas, J. L. Diffusion of mesoscopic probes in aqueous polymer solutions measured by fluorescence recovery after photobleaching. *Macromolecules* **2002**, *35*, 8111−8121.

(11) Kalathi, J. T.; Yamamoto, U.; Schweizer, K. S.; Grest, G. S.; Kumar, S. K. Nanoparticle diffusion in polymer nanocomposites. *Phys. Rev. Lett.* **2014**, *112*, 108301.

(12) Yamamoto, U.; Schweizer, K. S. Microscopic theory of the long-time diffusivity and intermediate-time anomalous transport of a nanoparticle in polymer melts. *Macromolecules* **2015**, *48*, 152−163.

(13) Cai, L.-H.; Panyukov, S.; Rubinstein, M. Mobility of Spherical Probe Objects in Polymer Liquids. *Macromolecules* **2011**, *44*, 7853−7863.

(14) Guo, H.; Bourret, G.; Lennox, R. B.; Sutton, M.; Harden, J. L.; Leheny, R. L. Entanglement-controlled subdiffusion of nanoparticles within concentrated polymer solutions. *Phys. Rev. Lett.* **2012**, *109*, 055901.

(15) Cukier, R. I. Diffusion of Brownian Spheres in Semidilute Polymer Solutions. *Macromolecules* **1984**, *17*, 252−255.

(16) Phillies, G. D. J.; Ullmann, G. S.; Ullmann, K.; Lin, T.-H. Phenomenological scaling laws for "semidilute" macromolecule solutions from light scattering by optical probe particles. *J. Chem. Phys.* **1985**, *82*, 5242−5246.

(17) Brochard Wyart, F.; de Gennes, P. G. Viscosity at small scales in polymer melts. *Eur. Phys. J. E: Soft Matter Biol. Phys.* **2000**, *1*, 93−97.

(18) Cai, L.-H.; Panyukov, S.; Rubinstein, M. Hopping diffusion of nanoparticles in polymer matrices. *Macromolecules* **2015**, *48*, 847−862.
(19) Degiorgio, V.; Mantegazza, F.; Piazza, R. Transient electric birefringence measurement of the persistence length of sodium polystyrene sulfonate. *Europhys. Lett.* **1991**, *15*, 75−80.
(20) Noda, I.; Tsuge, T.; Nagasawa, M. The intrinsic viscosity of polyelectrolytes. *J. Phys. Chem.* **1970**, *74*, 710−719.
(21) Boris, D. C.; Colby, R. H. Rheology of sulfonated polystyrene solutions. *Macromolecules* **1998**, *31*, 5746−5755.
(22) Colby, R. H. Structure and linear viscoelasticity of flexible polymer solutions: Comparison of polyelectrolyte and neutral polymer solutions. *Rheol. Acta* **2010**, *49*, 425−442.
(23) Senanayake, K. K.; Mukhopadhyay, A. Nanoparticle Diffusion within Dilute and Semidilute Xanthan Solutions. *Langmuir* **2019**, *35*, 7978−7984.
(24) Senanayake, K. K.; Shokeen, N.; Fakhrabadi, E. A.; Liberatore, M. W.; Mukhopadhyay, A. Diffusion of nanoparticles within a semidilute polyelectrolyte solution. *Soft Matter* **2019**, *15*, 7616−7622.
(25) Lopez, C. G. Entanglement Properties of Polyelectrolytes in Salt-Free and Excess-Salt Solutions. *ACS Macro Lett.* **2019**, 979−983.
(26) Broseta, D.; Leibler, L.; Lapp, A.; Strazielle, C. Universal properties of semi-dilute polymer solutions: A comparison between experiments and theory. *Europhys. Lett.* **1986**, *2*, 733−737.
(27) Wolff, C. Molecular Weight Dependence of the Relative Viscosity of Solutions of Polymers at the Critical Concentration. *Eur. Polym. J.* **1977**, *13*, 739−741.
(28) Crocker, J. C.; Grier, D. G. Methods of digital video microscopy for colloidal studies. *J. Colloid Interface Sci.* **1996**, *179*, 298−310.
(29) de Gennes, P.-G. *Scaling Concepts in Polymer Physics*; Cornell University Press: Ithaca, NY, 1979.
(30) Dobrynin, A. V.; Colby, R. H.; Rubinstein, M. Scaling Theory of Polyelectrolyte Solutions. *Macromolecules* **1995**, *28*, 1859−1871.
(31) Zimm, B. H. Dynamics of Polymer Molecules in Dilute Solution: Viscoelasticity, Flow Birefringence and Dielectric Loss. *J. Chem. Phys.* **1956**, *24*, 269−278.
(32) Rubinstein, M.; Colby, R. H. *Polymer Physics*; Oxford University Press: New York, 2003.
(33) Khorasani, F. B.; Poling-Skutvik, R.; Krishnamoorti, R.; Conrad, J. C. Mobility of nanoparticles in semidilute polyelectrolyte solutions. *Macromolecules* **2014**, *47*, 5328−5333.
(34) Ziębacz, N.; Wieczorek, S. A.; Kalwarczyk, T.; Fiałkowski, M.; Hołyst, R. Crossover regime for the diffusion of nanoparticles in polyethylene glycol solutions: Influence of the depletion layer. *Soft Matter* **2011**, *7*, 7181−7186.
(35) Mackie, J. S.; Meares, P. The diffusion of electrolytes in a cation-exchange resin membrane. II. Experimental. *Proc. R. Soc. London, Ser. A* **1955**, *232*, 510−518.
(36) Ogston, A. G. The spaces in a uniform random suspension of fibres. *Trans. Faraday Soc.* **1958**, *54*, 1754−1757.
(37) Ogston, A. G.; Preston, B. N.; Wells, J. D. On the Transport of Compact Particles Through Solutions of Chain-Polymers. *Proc. R. Soc. London, Ser. A* **1973**, *333*, 297−316.
(38) Mustafa, M. B.; Tipton, D. L.; Barkley, M. D.; Russo, P. S.; Blum, F. D. Dye Diffusion in Isotropic and Liquid Crystalline Aqueous (Hydroxypropyl)cellulose. *Macromolecules* **1993**, *26*, 370−378.
(39) Waggoner, R. A.; Blum, F. D.; MacElroy, J. M. D. Dependence of the Solvent Diffusion Coefficient on Concentration in Polymer Solutions. *Macromolecules* **1993**, *26*, 6841−6848.
(40) Amsden, B. An Obstruction-Scaling Model for Diffusion in Homogeneous Hydrogels. *Macromolecules* **1999**, *32*, 874−879.
(41) Holyst, R.; et al. Scaling form of viscosity at all length-scales in poly(ethylene glycol) solutions studied by fluorescence correlation spectroscopy and capillary electrophoresis. *Phys. Chem. Chem. Phys.* **2009**, *11*, 9025−9032.
(42) Kalwarczyk, T.; et al. Comparative analysis of viscosity of complex liquids and cytoplasm of mammalian cells at the nanoscale. *Nano Lett.* **2011**, *11*, 2157−2163.
(43) Kohli, I.; Mukhopadhyay, A. Diffusion of nanoparticles in semidilute polymer solutions: Effect of different length scales. *Macromolecules* **2012**, *45*, 6143−6149.
(44) Griffin, P. J.; Bocharova, V.; Middleton, L. R.; Composto, R. J.; Clarke, N.; Schweizer, K. S.; Winey, K. I. Influence of the Bound Polymer Layer on Nanoparticle Diffusion in Polymer Melts. *ACS Macro Lett.* **2016**, *5*, 1141−1145.
(45) Schumacher, G. A.; van de Ven, T. G. M. Brownian Motion of Charged Colloidal Particles surrounded by Electric Double Layers. *Faraday Discuss. Chem. Soc.* **1987**, *83*, 75−85.
(46) Seijo, M.; Pohl, M.; Ulrich, S.; Stoll, S. Dielectric discontinuity effects on the adsorption of a linear polyelectrolyte at the surface of a neutral nanoparticle. *J. Chem. Phys.* **2009**, *131*, 174704.
(47) Poling-Skutvik, R.; Krishnamoorti, R.; Conrad, J. C. Size-Dependent Dynamics of Nanoparticles in Unentangled Polyelectrolyte Solutions. *ACS Macro Lett.* **2015**, *4*, 1169−1173.
(48) Brochard, F.; de Gennes, P. G. Dynamical Scaling for Polymers in Theta Solvents. *Macromolecules* **1977**, *10*, 1157−1161.
(49) Won, J.; Onyenemezu, C.; Miller, W. G.; Lodge, T. P. Diffusion of Spheres in Entangled Polymer Solutions: A Return to Stokes-Einstein\Behavior. *Macromolecules* **1994**, *27*, 7389−7396.
(50) Lampo, T. J.; Stylianidou, S.; Backlund, M. P.; Wiggins, P. A.; Spakowitz, A. J. Cytoplasmic RNA-Protein Particles Exhibit Non-Gaussian Subdiffusive Behavior. *Biophys. J.* **2017**, *112*, 532−542.
(51) He, W.; Song, H.; Su, Y.; Geng, L.; Ackerson, B. J.; Peng, H. B.; Tong, P. Dynamic heterogeneity and non-Gaussian statistics for acetylcholine receptors on live cell membrane. *Nat. Commun.* **2016**, *7*, 11701.
(52) Jee, A.-Y.; Curtis-Fisk, J. L.; Granick, S. Nanoparticle Diffusion in Methycellulose Thermoreversible Association Polymer. *Macromolecules* **2014**, *47*, 5793−5797.
(53) Guan, J.; Wang, B.; Granick, S. Even Hard-Sphere Colloidal Suspensions Display Fickian Yet Non-Gaussian Diffusion. *ACS Nano* **2014**, *8*, 3331−3336.
(54) Wang, B.; Anthony, S. M.; Bae, S. C.; Granick, S. Anomalous yet Brownian. *Proc. Natl. Acad. Sci. U. S. A.* **2009**, *106*, 15160−15164.
(55) Wang, B.; Kuo, J.; Bae, S. C.; Granick, S. When Brownian diffusion is not Gaussian. *Nat. Mater.* **2012**, *11*, 481−485.
(56) Wong, I. Y.; Gardel, M. L.; Reichman, D. R.; Weeks, E. R.; Valentine, M. T.; Bausch, A. R.; Weitz, D. A. Anomalous diffusion probes microstructure dynamics of entangled F-actin networks. *Phys. Rev. Lett.* **2004**, *92*, 178101.
(57) Xue, C.; Zheng, X.; Chen, K.; Tian, Y.; Hu, G. Probing Non-Gaussianity in Confined Diffusion of Nanoparticles. *J. Phys. Chem. Lett.* **2016**, *7*, 514−519.
(58) Lee, J.; Grein-Iankovski, A.; Narayanan, S.; Leheny, R. L. Nanorod mobility within entangled wormlike micelle solutions. *Macromolecules* **2017**, *50*, 406−415.
(59) Xue, C.; Shi, X.; Tian, Y.; Zheng, X.; Hu, G. Diffusion of Nanoparticles with Activated Hopping in Crowded Polymer Solutions. *Nano Lett.* **2020**, *20*, 3895−3904.
(60) Pryamitsyn, V.; Ganesan, V. Dynamics of probe diffusion in rod solutions. *Phys. Rev. Lett.* **2008**, *100*, 128302.
(61) Clara-Rahola, J.; Brzinski, T. A.; Semwogerere, D.; Feitosa, K.; Crocker, J. C.; Sato, J.; Breedveld, V.; Weeks, E. R. Affine and nonaffine motions in sheared polydisperse emulsions. *Phys. Rev. E* **2015**, *91*, 010301.

https://dx.doi.org/10.1021/acs.langmuir.0c01402
Langmuir 2020, 36, 9153−9159